Anal. Methods Environ. Chem. J. 8 (2) (2025) 65-77

AMECJ

Research Article, Issue 2
Analytical Methods in Environmental Chemistry Journal
Journal home page: www.amecj.com/ir

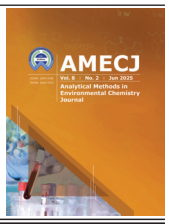

Analysis and photocatalytic degradation of methylene blue dye using a natural photosensitizer from Ruta extracts and UV-Vis spectrometry

Hichem Lettreuch[a,*], Asma Drioueche[b], and Hocine Boutoumi[b]

[a] *Université Yahia Farès de Médéa, Laboratoire Matériaux et Environnement, 26000 Médéa, Algérie*
[b] *Université Blida 1, Faculté de Technologie, Laboratoire de Génie Chimique (LGC), B. P. 270, Route de Soumaa, 09000Blida, Algérie*

ARTICLE INFO:

Received 15 Feb 2025
Revised form 19 Apr 2025
Accepted 20 May 2025
Available online 29 Jun 2025

Keywords:
UV-Vis spectroscopy,
Methylene blue,
ZnO,
Ruta montana and chalepensis L,
Photo-degradation,
Furocoumarins

ABSTRACT

Water treatment using sustainable methods is currently a major focus for researchers. In this context, the presented study explores an eco-friendly approach for removing harmful dyes from wastewater by utilizing extracts from the leaves of Ruta Montana L. and Ruta Chalepensis L. for the photodegradation of dye-contaminated water. The photo-catalytic performance of the obtained extracts and the pure xanthotoxin isolated from these extracts was investigated for methylene blue elimination using the photo-degradation process followed by UV-Vis spectroscopy. This method combines the power of sunlight with plant-derived photo-catalysts, especially furocoumarins known for their photochemical properties. The results of the UV-Vis measurement showed that the *Ruta chalepensis* extract exhibited better photo-degradation performance (24%) than *Ruta montana* extract (18%) at a concentration of 20 mg L^{-1}. In comparison, the pure xanthotoxin, the active ingredient, showed an interesting photo-degradation of dye (33%); this efficiency increases with increasing extract dose. The use of the Xanthotoxin/ZnO hetero system caused an improvement of the photo-degradation ability to (91%). These results were confirmed by the study of the kinetic of the dye degradation, where the hetero system Xanthotoxin/ZnO represents the highest values of the rate constant (k) and the correlation coefficients (R^2). Also, the xanthotoxin can be separated from the wastewater mixture by centrifugation, and spectroscopic analysis showed that the photo-degradation process did not alter the molecule.

1. Introduction

Water pollution is increasing daily, and its impact on human health [1,2], aquatic ecosystems [3], and biodiversity [4,5] is a serious threat. Industry represents the leading cause of water contamination due to various toxic chemicals, organic and inorganic substances like pesticides, pharmaceuticals, and dyes [6]. More than 10,000 tons of synthetic dyes are complex in structure and used in various industries, mainly in textile manufacturing [7]. The wastes of these industries can cause a direct or indirect danger to our environment if they are released without adequate treatment. For this reason, various chemical processes such as advanced oxidation [8], electrochemical degradation [9], and physical separation [10], such as filtration, membrane separation [11,12], and biological methods [13] for degradation of organic pollutants and water purification were investigated. Photo-degradation is of great interest because of

*Corresponding Author: Hichem Lettreuch
Email: hichemlet@yahoo.fr
https://doi.org/10.24200/amecj.v8.i02.1017

its efficiency and feasibility [14]; however, this process requires effective, biocompatible photo-catalysts with a high surface area [15]. The use of ionic liquids based on functionalized Carbone nanotubes [16,17] and several metals (Ag, Au) and oxides nanoparticles as photo-catalysts has been the object of different studies [18,19]; most applications use TiO_2 and ZnO in photo-degradation reactions [20-22], these catalysts were also used in junction [23,24]. Currently, the use of plant extracts for adsorption of dyes [25], and for green synthesis of nano-materials used in photo-catalytic degradation of organic pollutants is recommended for an environmentally friendly technology in order to minimize the danger of the chemicals used in the treatment of water [26]. Furocoumarins are a class of secondary metabolites produced by a variety of plants, consisting of a furan ring fused with a coumarin; (furan moiety fused at C_6 and C_7, respectively: linear psoralens and non-linear angelicins: furan moiety fused at C_7 and C_8, respectively) [27]. They have a lipophilic character and have limited solubility in water. The largest quantities of these compounds are found in the Apiaceae family, such as Ammi, parsnip [28,29], and in the *Rutaceae,* including all citrus fruits and *Ruta* species [30]. Furanocoumarins are used in phototherapy due to their photo-reactivity under UV light irradiation at 320–380 nm [31], the photosensitivity of these compounds allows them different applications [27, 29]. In the present study, *Ruta montana* L. and *Ruta chalepensis* L. extracts rich in furocoumarins, in addition to the pure xanthotoxin, were extracted and characterized with different spectroscopic methods and then tested for their photo-catalytic activity for the degradation of methylene blue under solar and artificial light.

2. Materials and Methods

2.1. Instrumental, Materials, and Reagents

The *Ruta montana* L. leaves were collected from Tipaza (70 km west of Algiers) in October 2022, and Ruta chalepensis L. from Ain defla (145 km southeast of Algiers) in October 2022. After being cleaned with distilled water, the *Ruta* species leaves were dried at room temperature. Methylene blue (MB) ($C_{16}H_{18}C_lN_3S$), a basic (cationic) dye, was purchased from SPECILAB, CAS No: 61-73-4, and ZNO (99.5%) (CAS No: 1314-13-2) from Riedel-de Haen. Petroleum ether 40-60 °C (CAS No: 8032-32-4) and ethanol (96%) (CAS No: 64-17-5) were purchased from Biochem (France). Ultraviolet-Visible spectra were measured in a quartz cuvette with a Shimadzu UV-1800 spectrophotometer, and the FT/ IR was registered on a BRUKER FT/IR spectrophotometer. The ^1H NMR and ^{13}C NMR spectra were recorded on a Bruker-Ascendi 400 MHz spectrometer in DMSO-d_6 (Sigma-Aldrich, Germany).

2.2. Extraction Process

Ruta montana L. and *Ruta chalepensis* L. leaves were extracted using a Soxhlet apparatus and petroleum ether as a solvent. The resulting extracts were concentrated under reduced pressure in a rotary evaporator. After the solvent evaporation, xanthotoxin was separated from the crude extracts as a white powder; the precipitate was filtered and recrystallized in ethanol.

2.3. Phytoscreening Tests

The *Ruta* extracts were tested for the presence of secondary metabolites like alkaloids, flavonoids, tannins, coumarins, and quinines using standard phytochemical procedures, according to the concept of Pandey and Tripathi [32]. The following test detected the alkaloids, flavonoids, tannins, and coumarins**.** *Ruta* extracts were contacted with Mayer's reagent (Potassium Mercuric Iodide). The formation of a yellow or brown precipitate indicates the presence of alkaloids as a detection test [32]. In a test tube, 1.0 mL of concentrated HCl was added to 1 mL of the extract, followed by a few magnesium turnings to detect Flavonoids. The appearance of red, orange, or pink color indicates the presence of flavonoids [33,34]. To detect Tannins, 2 mL of each extract was added to 0.5 mL of $FeCl_3$ (1%). The appearance of a greenish or blue-black color after incubation for 15 min at room temperature indicates the presence of tannins

[34,35]. Detection of coumarins was followed by 5 mL of each extract dissolved in 1-2 mL of hot distilled water, which was divided into two parts. Half of the volume was taken as a witness, and 0.5 mL 10% NH_4OH was added to the other volume; then, from each preparation, a spot was put on a filter paper and examined under UV light. The presence of coumarins was indicated by intense fluorescence [35,34].

2.4. Photocatalytic Degradation Procedure

The photocatalytic activity of Ruta Montana extract, Ruta chalepensis extract, ZnO, and xanthotoxin was tested by photodegradation of an aqueous solution of 20 mg L^{-1} methylene blue dye. The effect of adsorption of MB on the catalysts was determined by dispersing the catalyst to be tested in the MB solution, and putting it under continual stirring for 30 min in the dark. After the adsorption, the reactor is introduced under sunlight irradiation or artificial light using a SYLVANIA UV-A lamp (20 W) with stirring for 120 min. Samples are taken at different reaction times (15, 30, 60, 90, 120 minutes) using a piston pipette and placed in an EPPENDORF 5804 centrifuge at 5000 rpm for 10 min, then in quartz cells 1.0 cm thick, and then measuring the absorbance by the UV-Visible spectrophotometer. The results are illustrated (C⁄C0 =f(t)), with C:Concentration of the solution at t, C_0: the initial concentration of the MB solution (20mg L^{-1}), and t: time of irradiation.

3. Results and Discussion

3.1. Extraction

3.1.1.Phytochemical Screening

Table 1 represents the qualitative analysis of phytochemicals present in the petroleum ether extracts of *Ruta Montana* and *Ruta chalepensis.* The presented study revealed that flavonoids, coumarins, and tannins were the secondary metabolites found in the petroleum ether extracts of both Ruta Montana and Chalepensis. The most published articles recognized the presence of these phytochemicals in the *Ruta* species extracts [34, 35]. As shown in Table 1, the *Ruta montana* extract is richer in coumarin and tannins than Ruta chalepensis but richer in flavonoids. This is in line with previous studies where the apolar extract (petroleum ether, diethyl-ether) of *Ruta montana* contained a high yield of coumarins, essentially: bergapten, rutamarin, xanthotoxin, chalepensin [36].

3.1.2.Xanthotoxin characterization

After purification and recrystallization of xanthotoxin as previously purified [34], its chemical structure was elucidated using UV-Vis,

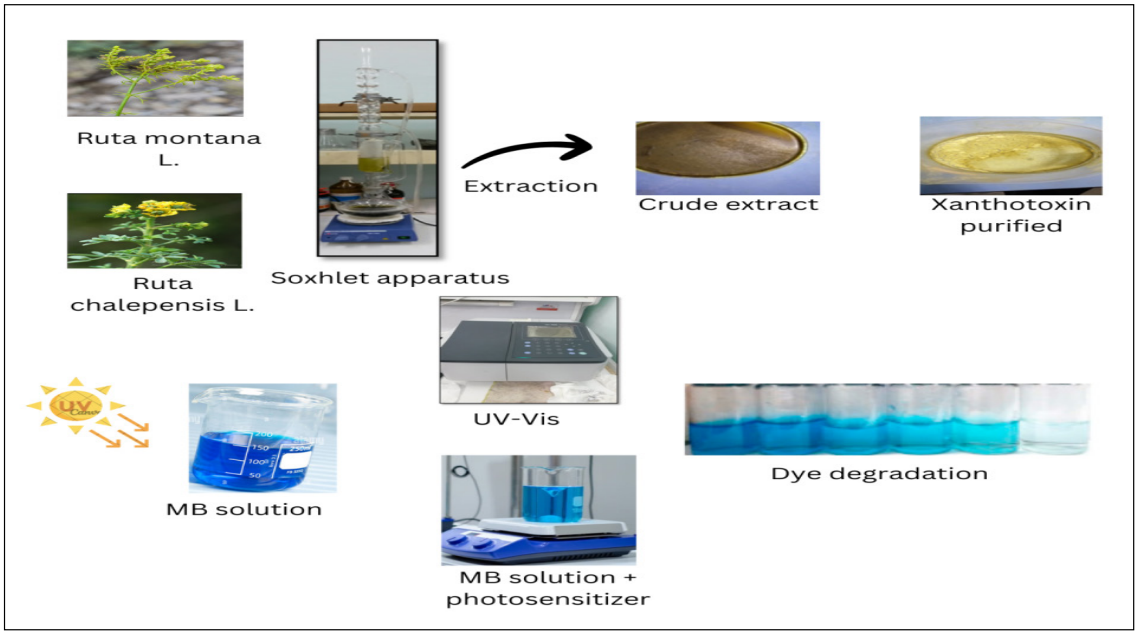

Fig.1. Extraction and photo-degradation procedure

Table 1. Phytochemical screening of *Ruta* species

Phyto-chemicals	Ruta montana L.	Ruta chalepensis L.
Alkaloids	-	-
Flavonoids	++	+++
Coumarins	+++	++
Tannins	+++	+

IR,^{1}H-NMR, and ^{13}C-NMR spectra. Xanthotoxin was characterized as a white powder, with mp: 145° C and Rf: $CH_3COOC_2H_5$/ C_6H_{12} (7:3 V/V) = 0,46. The UV-vis spectrum represents four bands at 215, 246-250, 294, and 346 nm (UV λmax). We can generally find these bands in the UV-Vis spectra of coumarins [37, 38]. The infrared spectrum (KBr) of xanthotoxin is characterized by the presence of characteristic peaks at: 3117 cm^{-1}(=CH_{arom}); 2951, 2917, 2848 cm^{-1}(-CH); 1705 cm^{-1}(C=O); 1681 cm^{-1}(C=C); 1332, 1150 cm^{-1}(C-O). These results are comparable to other methods [34]. The signals of the NMR H^1 and NMR C^{13} obtained and cited below were practically identical to those obtained by other researchers [39, 40].

NMR H^1 (DMSO-d$_6$,400 MHz): *δ/ppm: 4.20 (s, 3H, OCH_3), 6.44 (d, J=9.5 Hz, 1H, H-3), 7.10 (d, J=2.0 Hz,1H, H-4'), 7.67 (s, 1H, H-5), 8.13 (d, J=2,0 Hz, 1H, H-5'), 8.15 (d, J=10.0 Hz,1H, H-4).*

NMR C^{13}(DMSO-d$_6$,400 MHz): *δ/ppm: 61.58 (9-OCH_3), 107.72 (C-4'), 114.01 (C-5), 114.64 (C-3), 116.92 (C-6), 125.96 (C-4a), 132.51 (C-8), 142.26 (C-8a), 145.72 (C-4), 147.32 (C-2), 147.89 (C-5'), 160.18 (C-7).*

3.2. Photo-degradation study of MB dye

The present study examined the potential of the Ruta montana L. extract, Ruta chalepensis L. extract, and pure xanthotoxin for photocatalytic degradation of methylene blue under direct sunlight and artificial light.

3.2.1.Effect of Ruta extracts and pure xanthotoxin

The absorbance spectra of methylene blue solutions containing 20 mg L^{-1} of *Ruta* extracts under sunlight are shown in Figure 2. It is clear that without using Ruta extracts, there was no significant degradation over 2 hours, whereas in the presence of Ruta montana L. and Ruta chalepensis L. extracts, the absorbance steadily lowers with increasing exposure time. Ruta extracts caused a degradation of approximately 20-25% of methylene blue after 2 hours of exposition under sunlight, representing a relatively medium photocatalytic activity. This comparative study observed that the Ruta chalepensis extract exhibited better photo-degradation performance (24%) than the Ruta montana L. extract (18%). This photocatalytic activity is relative to the presence of photoactive molecules in our extracts, especially furocoumarins, which are known for their photosensitizing properties [27]. It has been reported that some essential oils and plant extracts rich in furocoumarins, such as the essential oils of Citrus bergamia, Citrus limonum, Citrus paradisi, and Citrus sinensis, are photoactive and show solar water disinfectant properties [41].
These results led us to test the ability of the pure furocoumarins; in this context, the xanthotoxin was isolated from the apolar extract of both plants by purification and crystallization as already shown [34]. We have obtained a yield of 0.4% from *Ruta montana* L extract and 0.31% of xanthotoxin from *Ruta chalepensis* extract**.** The effect of initial xanthotoxin dose variation on photo-catalytic degradation efficiency was examined by changing its concentration at a constant dye dose C= 20 mg L^{-1} and pH= 7.4 under artificial light using a UV-A lamp. Figure 3 shows xanthotoxin showed an interesting photodegradation at low concentration. It is clear that the degradation efficiency increase with increasing xanthotoxin dose, where 20 mg L^{-1} of xanthotoxin caused a degradation of approximately 33% of methylene blue dye. In contrast, 40 mg L^{-1} degraded 59% of dye; these results are comparable with photo-degradation of dyes using ZnO at 40 mg L^{-1} [24].

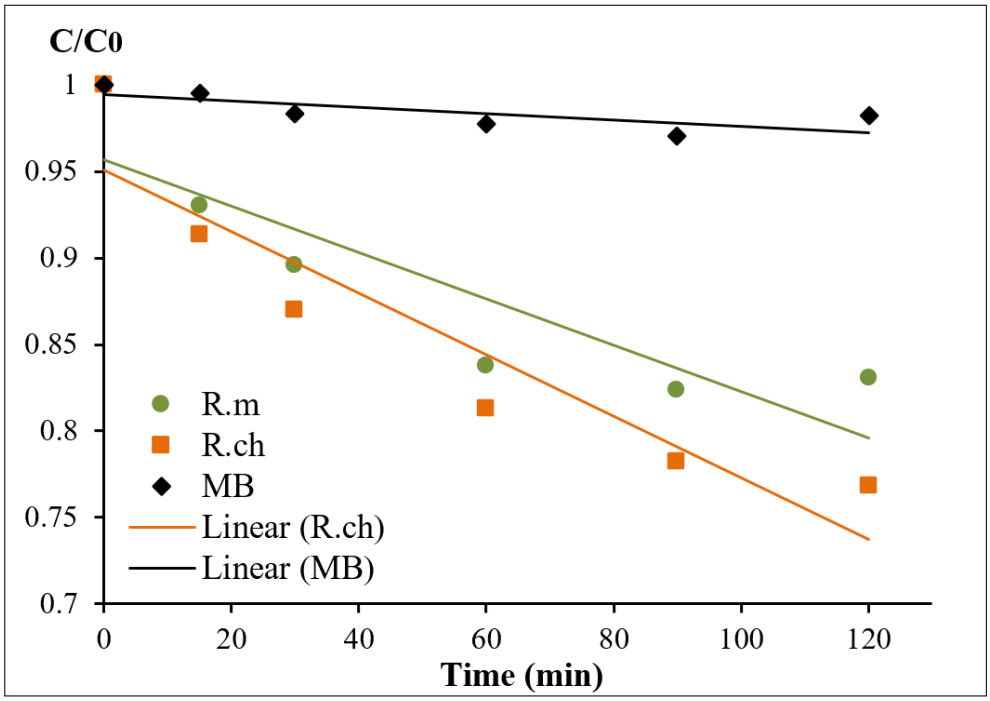

Fig. 2. Degradation of methylene blue (MB) dye in the presence of 20 mg L^{-1} of the Ruta montana L. extract (R.m) and Ruta chalepensis L. extract (R.ch) under sunlight

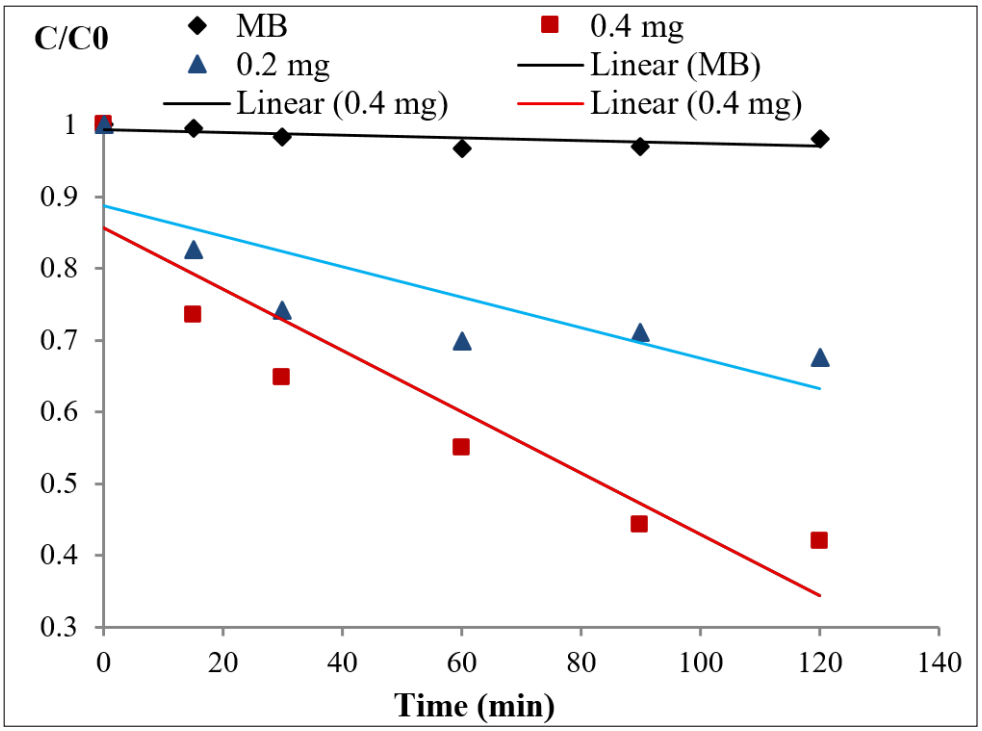

Fig. 3. Effect of xanthotoxin concentration on Methylene blue (MB) degradation, pH=7.4 under UV-A light (20 W).

3.2.2.Mechanism

Xanthotoxin is a natural furocoumarin having photoactive properties photosensitize (320-400 nm) UV by way of Type I (sensitizer-substrate) and Type II (sensitizer-oxygen) mechanisms [42], for these reasons it represents interesting photo-degradation capabilities, this molecule is activated by absorbing photons from natural or artificial light and pass from the ground state to the excited state, and transfer energy to the oxygen by returning to the ground state which pass to the excited state and transfer an electron to the oxygen dissolved in water to produce singlet oxygen ($^1O_2$) and hydroxyl radicals, which attack the dye molecules and involves breaking down conjugated systems in the dye structure.

Catalyst Regeneration

The xanthotoxin used in adsorption can be regenerated after photo-degradation of dye using centrifugation and precipitation, and we can filter it from the treatment water solution, as it is an organic product. Figure 4a and b, which represent the IR spectra of xanthotoxin before and after photo-degradation, show that the photo-degradation process did not alter the molecule, and the IR spectrum was not modified. Also, the UV-Vis spectrum and H^1 NMR spectra of Xanthotoxin and the C^{13} NMR spectra of Xanthotoxin were shown in Figures 4c-e.

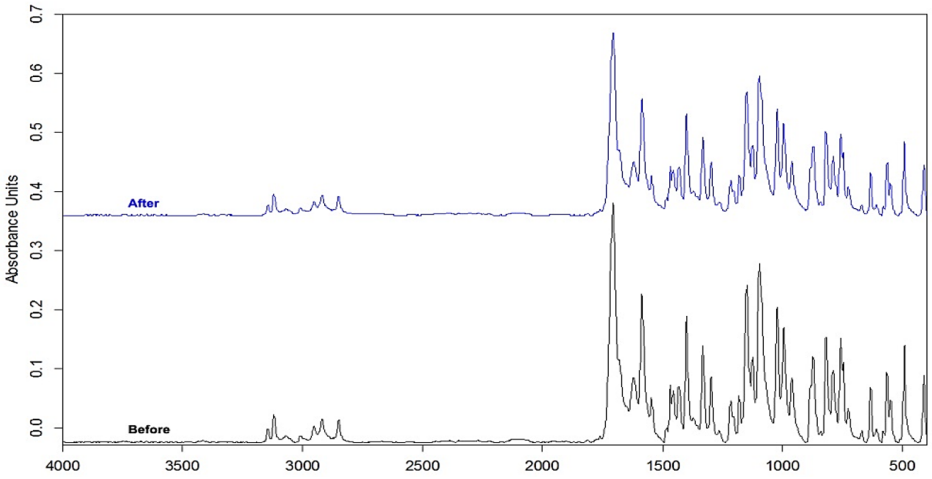

Fig. 4a. Comparing the infrared spectrum of Xanthotoxin before and after adsorption.

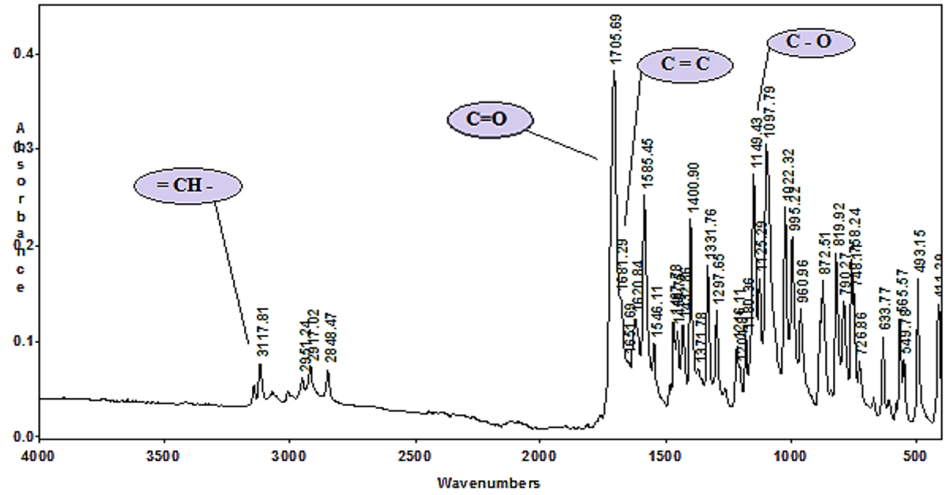

Fig.4 b. Infra-red spectra of Xanthotoxin

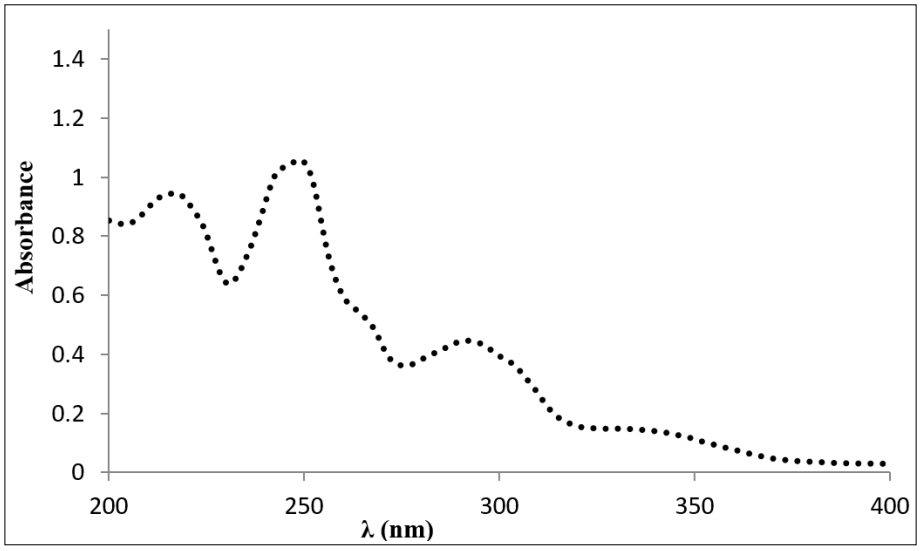

Fig. 4c. UV-Visible spectra of Xanthotoxin

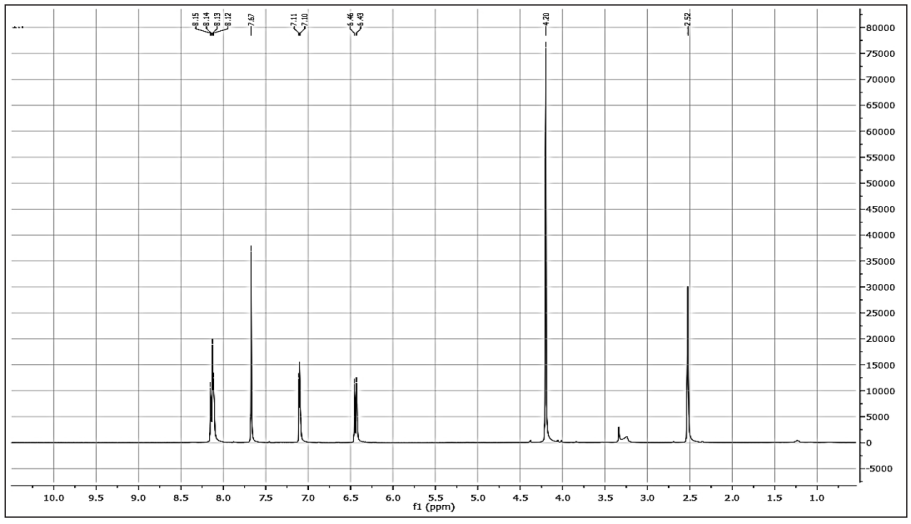

Fig.4d. H^1 NMR spectra of Xanthotoxin

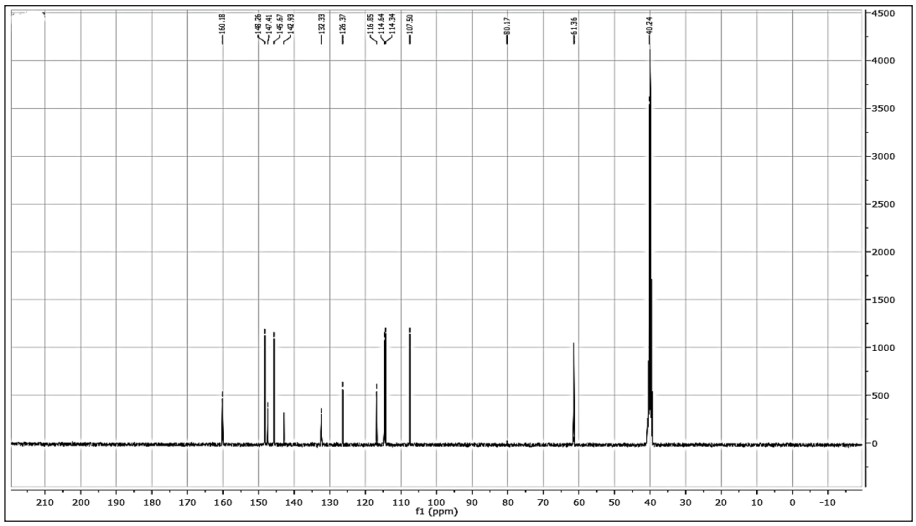

Fig.4e. C^{13} NMR spectra of Xanthotoxin

3.2.3.Hetero-system study

The photo-catalytic activity of different catalysts and extracts for the photo-degradation of methylene blue is presented in Figure 5. The presented results show that the photocatalytic activity of ZnO at 40 mg L^{-1} was (60 %), this is comparable with the previous researches of ZnO [24], so in order to improve this activity; the photo-sensitizer Xanthotoxin is added gradually to determine the best ratio in the mixture of Xanthotoxin/ZnO. The photodegradation of methylene blue has been increased to 91 % using the hetero system Xanthotoxin/ZnO.

The calculated degradation efficiency of MB, represented in Figure 6, shows that 60mg/L of heterosystem Xanthotoxin /ZnO, with a ratio of (33.33%: 66.66%), means the highest photo-degradation ability. It was reported that the photocatalytic activity of ZnO increases by using mixtures of photocatalysts [43,44]. These results are compared with the effects of other catalysts studied for their photocatalytic activity and illustrated in Table 2.

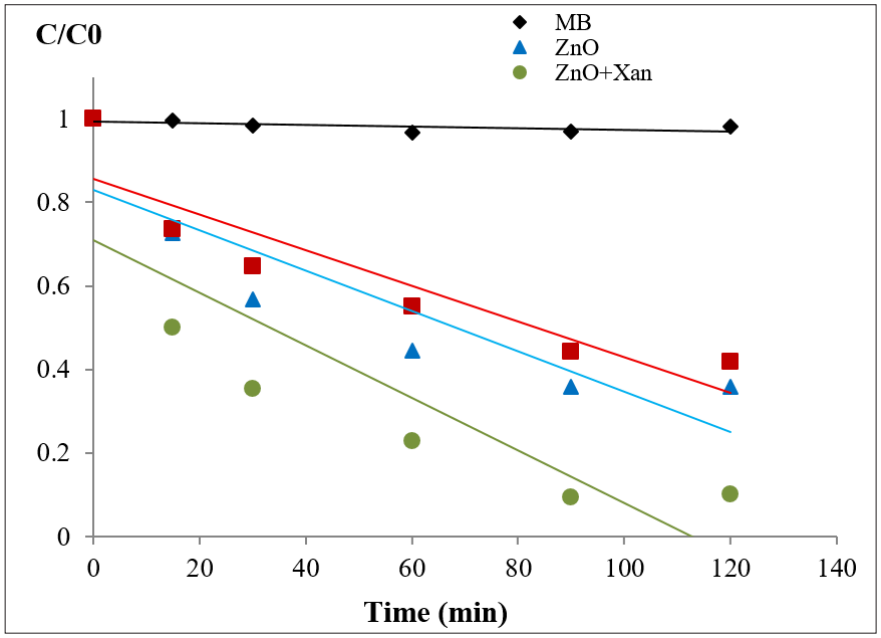

Fig. 5. Variation of absorbance of methylene blue (MB) dye in the presence of 20 mg of xanthotoxin (Xan), 40 mg of ZnO, and the combination of 60 mg/L of ZnO+Xan with a (66.66%:33.33%) ratio under UV-A light (20 W) and pH=7.4.

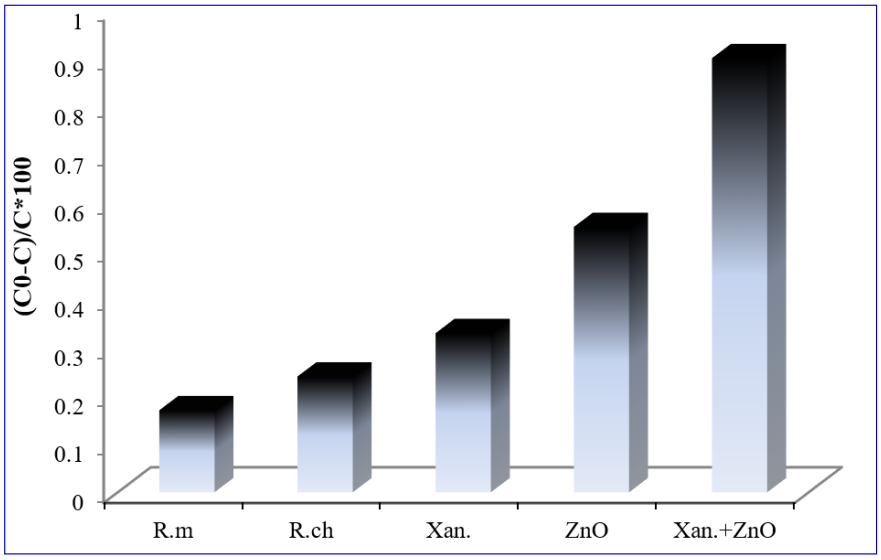

Fig. 6. Histogram showing the photo-activity of *Ruta* extracts (20mg/L), ZnO (40 mg L^{-1}), Xanthotoxin (40 mg/L), and their combination in hetero system (Xan+ZnO), MB (20 mg L^{-1}) at pH=7.4 under UV-A light (20 W)

Table 2. Effects of catalyst loading on photocatalytic degradation of some pollutants in wastewaters

Catalyst	Pollutant	Amount of catalyst	Degradation (%)	References
Xanthotoxin /ZnO	Methylene Blue	40 mg L^{-1}	91%	This work
CuO/TiO2-graphene	Methylene Blue	30 mg per 100 mL^{-1}	80%	[45]
CuO/ZnO	Amoxicilline	0.5g L^{-1}	90%	[24]
Ag/ZnO	Methyl Orange	30 mg per 100 mL^{-1}	90%	[44]
Bi_2O_3/TiO_2	Formaldehyde	-	95%	[21]

3.2.4. Degradation kinetics

The kinetic constants of dye photo-degradation were estimated according to first-order kinetics, and the plot ofVersus time for all samples (Fig.7). C_0 is the initial concentration of the MB solution, and C_t is the concentration of the MB solution at time t.

Degradation rate constants (k) and linear regression coefficients (R^2) determined from the straight-line graph using linear fitting = kt are presented in Table 3. The values of k and R^2 confirm that the Xanthotoxin /ZnO hetero system exhibits improved photo-catalytic performance, where the highest values were obtained (k=0.019 and R^2=0.970) compared with the other photosensitizers and catalysts tested.

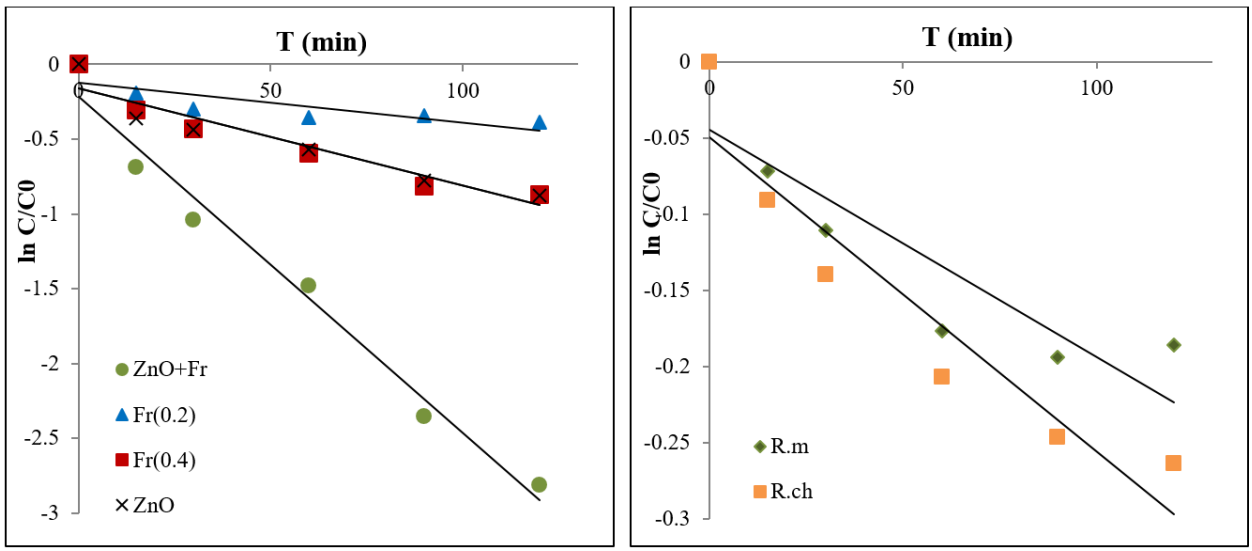

Fig. 7. The linear plot of vs. time for methylene blue (MB) dye degradation in the presence of 20 mg L^{-1} of the *Ruta montana* extract (R.m) and *Ruta chalepensis* extract (R.ch), xanthotoxin (Fr), 40 mg of ZnO, and 60 mg L^{-1} of the combination (ZnO+Fr)

Table 3. Photocatalytic reaction parameters

Type of catalyst	Rate constant (k) min^{-1}	R^2
Ruta montana L. extract	0.001 ±	0.800
Ruta chalepensis L. extract	0.002 ±	0.888
Xanthotoxin	0.006 ±	0.915
ZnO	0.006 ±	0.881
ZnO-Xanthotoxin	0.019 ±	0.970

4. Conclusion

The presented study investigated a sustainable and simple method for photo-degrading methylene blue dye from apolar Ruta extracts. Ruta montana L. and Ruta chalepensis L. extracts are rich in secondary metabolites like flavonoids, tannins, and especially coumarins, which are natural photosensitizers. The xanthotoxin, known for its photosensitizer properties, was isolated from the Ruta extracts, and its chemical structure was confirmed using different spectroscopic methods. The *Ruta* extracts and the pure xanthotoxin have shown the ability for photo-degradation of methylene blue dye studying by UV-Vis spectroscopy at a concentration of 20 mg L^{-1}, where the *Ruta chalepensis* extract exhibited better photo-degradation performance (24%) than *Ruta montana* extract with (18%) of degradation, whereas the pure xanthotoxin showed more efficiency (33%) at the same concentration and a comparative photo-degradation results as ZnO (60%) with 40 mg L^{-1}; on the other hand the use of the Xanthotoxin /ZnO hetero system caused an increased to (91%) in the photo-degradation ability. After photo-degradation, xanthotoxin was separated from the mixture by centrifugation, and spectroscopic analysis showed that the process did not alter the molecule.

5. References

[1] L. Lin, H. Yang, X. Xu, Effects of water pollution on human health and disease heterogeneity: A review, Front. Environ. Sci.,10 (2022) 880246. https://doi.org/10.3389/fenvs.2022.88024

[2] W.M. Warren-Vega, A. Campos-Rodríguez, A. I. Zárate-Guzmán, L. A. Romero-Cano, A current review of water pollutants in the American continent: trends and perspectives in detection, health risks, and treatment technologies. Int. J. Environ. Res. Public Health, 20 (2023) 4499. https://doi.org/10.3390/ijerph20054499

[3] I. Bashir, F.A. Lone, R. A. Bhat, S. A. Mir, Z. A. Dar, S. A. Dar, Concerns and threats of contamination on aquatic ecosystems, Bioremediation and Biotechnology, Springer, pp. 1–26, 2020. https://doi: 10.1007/978-3-030-35691-0_1

[4] R. Lylia, H. Ramzi, K. Hichem, M. Djemoi, S. Menouar, Groundwater quality in two Semi-Arid areas of Algeria: Impact of water pollution on biodiversity, J. Biores. Manag., 7 (2020) 16-34. https://doi.org/10.35691/JBM.0202.0137

[5] M. Dulsat-Masvidal, C. Ciudad, O. Infante, R. Mateo, S. Lacorte, Water pollution threats in important bird and biodiversity areas from Spain, J. Hazard. Mater., 448 (2023) 130938. https://doi.org/10.1016/j.jhazmat.2023.130938

[6] P. Chowdhary, R. N. Bharagava, S. Mishra, N. Khan, Role of industries in water scarcity and its adverse effects on environment and human health, publisher Springer Singapore, Environ. Concerns Sustain. Dev., pp. 235–256, 2019. https:// doi:10.1007/978- 981-13-5889-0_12

[7] R. Al-Tohamy, S. S. Ali, F. Li, K. M. Okasha, Y. A. G. Mahmoud, T. Elsamahy, H. Jiao, Y. Fu, J. Sun, A critical review on the treatment of dye-containing wastewater: Ecotoxicological and health concerns of textile dyes and possible remediation approaches for environmental safety, Ecotoxicol. Environ. Saf., 231 (2022) 113160. https://doi.org/10.1016/j.ecoenv.2021.113160

[8] D. Dimitrakopoulou, I. Rethemiotaki, Z. Frontistis, P.X. Nikolaos, D. Venieri, D. Mantzavinos, Degradation, mineralization and antibiotic inactivation of amoxicillin by UV-A/TiO_2photocatalysis, J. Environ. Manag., 98 (2012) 168-174. https://doi.org/10.1016/j.jenvman.2012.01.010

[9] D. K. Sarfo, A. Kaur, D. L. Marshall, A. P. O'Mullane, Electrochemical degradation and mineralisation of organic dyes in aqueous nitrate solutions, Chemosphere, 316 (2023) 137821. https://doi.org/10.1016/j.chemosphere.2023.137821

[10] J. Tian, X. Chen, Physical separation:

reuse pollutants and thermal energy from water, Water, 15 (2023) 1196. https://doi.org/10.3390/w15061196

[11] A. Giacobbo, A. M. Bernardes, Membrane separation process in wastewater and water purification, Membranes, 12 (2022) 259. https://doi.org/10.3390/membranes12030259

[12] H. Panyang, Z. Fengye, Z. Yaojun, C. Hao, Multifunctional fly ash-based GO/geopolymer composite membrane for efficient oil-water separation and dye degradation, Ceram. Int., 49 (2023) 1855-1864. https://doi.org/10.1016/j.ceramint.2022.09.149

[13] S. Arvind, B. P. Dan, M . Akbar, A. Alaa, H. Shafiul, Y. Taeho, S. Neha, K. G. Vijai, Biological remediation technologies for dyes and heavy metals in wastewater treatment: New insight, Bioresour. Technol., 343 (2022) 126154. https://doi.org/10.1016/j.biortech.2021.126154

[14] M. Saeed, M. Muneer, Photocatalysis: an effective tool for photodegradation of dyes-A review, Environ. Sci. Pollut. Res., 29 (2022) 293–311. https://doi.org/10.1007/s11356-021-16389-7

[15] M. S. H. Bhuiyan, M. Y. Miah, S. C. Paul, T. D. Aka, O. Saha, M. M. Rahaman, M. J. I. Sharif, O. Habiba, M. Ashaduzzaman, Green synthesis of iron oxide nanoparticle using Carica papaya leaf extract: application for photocatalytic degradation of remazol yellow RR dye and antibacterial activity, Heliyon, 6 (2020) e04603. https://doi.org/10.1016/j.heliyon.2020.e04603

[16] S. Teimoori, A. H. Hassani, New extraction of toluene from water samples based on nano-carbon structure before determination by gas chromatography, Int. J. Environ. Sci. Technol., 20 (2023) 6589–6608. https://doi.org/10.1007/s13762-023-04906-9

[17] S. Teimoori, A. H. Hassani, M. Panahi, N. Mansouri, Rapid extraction of BTEX in water and milk samples based on functionalized MWCNTs by dispersive homogenized-micro-solid phase extraction, Food Chem., 421 (2023) 136229. https://doi.org/10.1016/j.foodchem.2023.136229

[18] K. Ö. Hamaloglu, E. Sag, A. Tuncel, Bare, gold and silver nanoparticle decorated, monodisperse-porous titaniamicrobeads for photocatalytic dye degradation in a newly constructed microfluidic, photocatalytic packed-bed reactor, J. Photochem. Photobiol. A: Chem., 332 (2017) 60–65. https://doi.org/10.1016/j.jphotochem.2016.08.015

[19] K. R. Ahammed, M. Ashaduzzaman, S. C. Paul, M. R. Nath, S. Bhowmik, O. Saha, M. Rahaman, S. Bhowmik, T. D. Aka, Microwave assisted synthesis of zinc oxide (ZnO) nanoparticles in a noble approach: utilization for antibacterial and photocatalytic activity, SN Appl. Sci., 2 (2020) 955. https://doi.org/10.1007/s42452-020-2762-8

[20] S. Teimoori, An immobilization of aminopropyl trimethoxysilane-phenanthrene carbaldehyde on graphene oxide for toluene extraction and separation in water samples, Chemosphere, 316 (2023) 137800. https://doi.org/10.1016/j.chemosphere.2023.137800

[21] M. M. Asl, F. Atabi, Functionalized graphene oxide with bismuth and titanium oxide nanoparticles for efficiently removing formaldehyde from the air by photocatalytic degradation–adsorption process, J. Anal. Test., 7 (2023) 444-458. https://doi.org/10.1007/s41664-023-00272-0

[22] M. Mohammadi Asl, N. Mansouri, S. A. R. Haji Seyed Mirzahosseini, F. Atabi, Simultaneity comparative evaluation of toluene removal from the air by adsorption and UV semi-degradation-based adsorption procedure, Int. J. Environ. Sci. Technol., 21 (2024) 6677-6694. https://doi.org/10.1007/s13762-024-05503-0

[23] E. S. Elmolla, M. Chaudhuri, Photocatalytic degradation of amoxicillin, ampicillin, and cloxacillin antibiotics in aqueous solution using UV/TiO_2 and UV/H_2O_2 / TiO_2 photocatalysis, Desalination, 252 (2010) 46–52. https://doi.org/10.1016/j.

desal.2009.11.003

[24] Y. Belaissa, D. Nibou, A. A. Assadi, B. Bellal, M. Trari, A new hetero-junction *p*-CuO/ *n*-ZnO for the removal of amoxicillin by photocatalysis under solar irradiation, J. Taiwan Inst. Chem. Eng., 68 (2016) 254-265. https://doi.org/10.1016/j.jtice.2016.09.002

[25] S. T. Al-Asadi, F. F. Al-Qaim, H. F. S. Al-Saedi, I. F. Deyab, H. Kamyab, S. Chelliapan, Adsorption of methylene blue dye from aqueous solution using low-cost adsorbent: kinetic, isotherm adsorption, and thermodynamic studies, Environ. Monit. Assess., 195 (2023) 676. https://doi.org/10.1007/s10661-023-11334-2

[26] S. Ying, Z. Guan, P.C. Ofoegbu, P. Clubb, C. Rico, F. He, J. Hong, Green synthesis of nanoparticles: Current developments and limitations, Environ. Technol. Innov., 26 (2022) 102336. https://doi.org/10.1016/j.eti.2022.102336

[27] H. Bitterling, P. Lorenz, W. Vetter, D. R. Kammerer, F. C. Stintzing, Photo-protective effects of selected furocoumarins on *β*-pinene, *R*-(+)-limonene and *γ*-terpinene upon UV-A irradiation, J. Photochem. Photobiol. A: Chem., 424 (2022) 113623. https://doi.org/10.1016/j.jphotochem.2021.113623

[28] A. Balkrishna, V. Arya, I. Prakash Sharma, Anti-cancer and anti-inflammatory potential of furanocoumarins from *Ammi majus* L, Bentham Science publisher book, Anti-Cancer Agents in Medicinal Chemistry, 22 (2022) 1030-1036. https://dx.doi.org/10.2174/1871520621666210824113128

[29] H. M. Kenari, G. Kordafshari, M. Moghimi, F. Eghbalian, TaherKhani D, Review of pharmacological properties and chemical constituents of *Pastinaca sativa,* J. Pharmacopunct., 24 (2021) 14-23. https://doi.org/10.3831/KPI.2021.24.1.14

[30] S. Bergheul, M. Limones-Méndez, J. Grosjean, A. Hehn, A. Olry, A. Berkani, Comparative study of the production of coumarins and furanocoumarins in three Ruteae species, India. J. Nat. Prod. Resour., 10 (2019)137-142. https://doi.org/10.56042/ijnpr.v10i2.21358

[31] M. A. Pathak, D. M. Krämer, Photosensitization of skin *in vivo* by furocoumarins (psoralens), Biochim. Biophys. Acta, 195 (1969) 197-206. https://doi.org/10.1016/0005-2787(69)90616-9

[32] A. Pandey, S. Tripathi, Concept of standardization, extraction and pre phytochemical screening strategies for herbal drug, J. Pharmacogn. Phytochem., 2 (2014) 115-119. https://www.phytojournal.com/archives/2014/vol2issue5/PartB/11.1.pdf

[33] Y. Karumi, P. A. Onyeyili, V. O. Ogugbuaja, Identification of actives principles of M. balsamia (Balsam Apple), leaf extract, J. Med. Sci.,4 (2004) 179-182. https://doi.org/10.3923/jms.2004.179.182

[34] A. Drioueche, H. Boutoumi, H. Lettreuch, Antimicrobial activity of xanthotoxin isolated from *Ruta montana*L, extract and effect of harvesting time on its content, J. Mater. Environ. Sci., 12 (2021) 974-983. https://www.jmaterenvironsci.com/

[35] S. Dubale, D. Kebebe, A. Zeynudin, N. Abdissa, S. Suleman, Phytochemical screening and antimicrobial activity evaluation of selected medicinal plants in Ethiopia, J. Exp. Pharmacol., 15 (2023) 51–62. https://doi.org/10.2147/JEP.S379805

[36] N. Benkhaira, S. I. Koraichi, K. Fikri-Benbrahim, *Ruta montana* (L.) L.: An insight into its medicinal value, phytochemistry, biological properties, and toxicity, J. Herbmed. Pharmacol., 11 (2022) 305-319. https://doi.org/10.34172/jhp.2022.36

[37] G. Surico, L. Varvaro, M. Solfrizzo, Linear furocoumarin accumulation in celery infected with *Erwinia carotovora,* J. Agr. Food Chem., 35 (1987) 406-409. https://doi.org/10.1021/jf00075a030

[38] R.D.H. Murray, J. Mendez, S.A. Brown, The natural coumarins, occurrence, chemistry and

biochemistry, Britistol, John Wiley & Sons Ltd,1982. https://www.wiley.com/en-ca

[39] N. Finkelstein, C.F. Albrecht, P.P. Van Jaarsveld, Isolation and structure elucidation of xanthotoxin, a phototoxic furanocoumarin, from *Peucedanum galbanum,* S. Afr. J. Bot., 59 (1993) 81 – 84. https://doi.org/10.1016/S0254-6299(16)30778-5

[40] S E. Sajjadi, P. Noorozi, Isolation and identification of Xanthotoxine (8-methoxypsoralen) from the Fruits of *Heracleum persicum* Desf. Ex Fischer, Res. Pharm. Sci., 2 (2007) 13-16. http://rps.mui.ac.ir/index.php/jrps/article/view/21/19

[41] T. M. Sunda, K. Ngbolua, Contribution to the study of water disinfection by photosensitization with plants extracts: case of citrus limonum, citrus paradisi and citrus reticulate coumarin extracts, Int. J. Innov. Appl. Stud., 23 (2018) 89-94. https://ijias.issr-journals.org/

[42] L. I. Grossweiner, Mechanisms of photosensitization by furocoumarins, Natl. Cancer Inst. Monogr., 66 (1984) 47-54. https://pubmed.ncbi.nlm.nih.gov/6397692/

[43] A. Rafiq, M. Ikram, S. Ali, F. Niaz, M. Khan, Q Khan, M. Maqbool, Photocatalytic degradation of dyes using semiconductor photocatalysts to clean industrial water pollution, J. Ind. Eng. Chem., 97 (2021) 111-128. https:// doi.org/ 10.1016/ j.jiec.2021.02.017

[44] T. Chen, Y. Zheng, J.-M. Lin, G. Chen, Study on the photocatalytic degradation of methyl orange in water using Ag/ZnO as catalyst by liquid chromatography electrospray ionization ion-trap mass spectrometry, J. Am. Soc. Mass Spectrom., 19 (2008) 997-1003. https://doi.org/10.1016/j.jasms.2008.03.008

[45] Y. Fang, R.Wang, G. Jiang, CuO/TiO_2 nanocrystals grown on graphene as visible-light responsive photocatalytic hybrid materials, Bull. Mater. Sci., 35 (2012) 495–499. https:// doi.org/ 10.1007/ s12034-012-0338-y